Fractal Metamaterial Absorber with Three-Order Oblique Cross Dipole Slot Structure and its Application for In-Band RCS Reduction of Array Antennas

Sijia LI, Xiangyu CAO, Jun GAO, Yuejun ZHENG, Di ZHANG, Hongxi LIU

Information and Navigation College, Air Force Engineering University, 710077, Xi'an, China

lsj051@126.com, xiangyucaokdy@163.com, gjgj9694@163.com, erikzhengyang@126.com, dee19910330@163.com, hongxi_liu517@163.com

Abstract. *To miniaturize the perfect metamaterial absorber, a fractal three-order oblique cross dipole slot structure is proposed and investigated in this paper. The fractal perfect metamaterial absorber (FPMA) consists of two metallic layers separated by a lossy dielectric substrate. The top layer etched a three-order oblique fractal-shaped cross dipole slot set in a square patch and the bottom one is a solid metal. The parametric study is performed for providing practical design guidelines. A prototype with a thickness of 0.0106λ (λ is the wavelength at 3.18 GHz) of the FPMA was designed, fabricated, measured, and is loaded on a 1×10 guidewave slot array antennas to reduce the in-band radar cross section (RCS) based on their surface current distribution. Experiments are carried out to verify the simulation results, and the experimental results show that the absorption at normal incidence is above 90 % from 3.17 to 3.22 GHz, the size for the absorber is 0.1λ × 0.1λ, the three-order FPMA is miniaturized 60 % compared with the zero-order ones, and the array antennas significantly obtain the RCS reduction without the radiation deterioration.*

Keywords

Guidewave slot array antennas, fractal perfect metamaterial absorber, surface current distribution, RCS reduction.

1. Introduction

Radar cross section reduction (RCSR) of the antennas has been a topic of immense strategic interest for the researchers. For out-of-band frequencies, it is well known that the RCS of antenna/array can be significantly reduced by placing the periodic resistive surface (PRS) [1], [2] and suitably shaped band-pass radome, such as frequency selective surfaces (FSS) [3], [4]. However, when the radome is transparent, no RCS reduction of the antenna will significantly take place for in-band frequencies.

Nowadays, the metamaterial absorber has been paid attention to for in-band RCS reduction. In [5], the application of electromagnetic band-gap (EBG) radar absorbing material loaded with lumped resistances to ridged waveguide slot antenna array to reduce its in-band RCS was investigated, in which the lumped resistive elements were used to better match the impedance of free space, and as the chief contributor of absorption. The design idea is different from this work in [5]. In [6], an artificial magnetic conductor (AMC) and perfect electric conductor (PEC) surface were combined together for in-band RCS reduction and radiation improvement of waveguide slot antenna based on the principle of passive cancellation. In [7], two different AMCs were analyzed for ultra-thin and broadband RAM design. In [8], the reflection characteristic of a composite planar AMC surface has been investigated and fabricated for broadband RCS reduction. Similarly, a broadband RCS reduction for a waveguide slot antenna with orthogonal array of CSRR-AMC is presented in [9]. However, it is obvious that the RCS is reduced in boresight direction but increased in other directions in [6]-[10]. Perfect metamaterial absorber (PMA) with the ultrathin structure and the near-unity absorptivity was firstly proposed and demonstrated by Landy et. al. in [11], which has become an important aspect in the research of metamaterials. Later, to achieve polarization-insensitive absorption, wide incident angle absorption, broadband absorption, and multi-band absorption, many researchers make several efforts on the PMAs [12-20]. In 2013, a perfect metamaterial absorber with wide-angle and polarization-insensitive absorption was presented for RCS reduction of waveguide slot antenna in [16]. The maximum absorptivity of this absorber is 99.8 % with a full width at half maximum (FWHM) of 220 MHz. Then, a perfect metamaterial absorber (PMA) is applied for RCS reduction of a circularly polarized tilted beam antenna in [17]. But these PMAs cannot be directly used for the reduction of the guidewave slot array antennas (GSAAs) due to the large structure and radiation deterioration, especially the gain reduction.

In this paper, an ultrathin and miniaturized FPMA with the three-order oblique cross dipole slot (TOOCDS) structure is presented and investigated for its application

for RCS reduction of the 1×10 GSAAs without radiation property deterioration. Experimental results show that the absorption is above 90 % from 3.17 to 3.22 GHz at normal incidence and the size of the absorber is 0.1λ × 0.1λ. The three-order FPMA is miniaturized 60 % compared with the zero-order ones. The FPMA is loaded on the array antennas to reduce the RCS according to their surface current distribution. And the simulated results indicate that the array antennas significantly obtain the RCS reduction without the radiation deterioration.

2. Design and Analysis of FPMA

Fig. 1(a), 1(b) and 1(c) show the geometry of the ultra-thin and miniaturized FPMA, which is composed of two metallic layers separated by a lossy dielectric substrate. The top layer etched a fractal-shaped TOOCDS set in a square patch and the bottom one is a solid metal. The metal is copper with the conductivity of 5.8×10^7 S/m. FR4 is used as the substrate with the relative permittivity of 4.4 and loss tangent of 0.02, respectively. The absorber structure was simulated and optimized using HFSS 14.0 by considering a unit cell. Optimized parameters are shown in Fig. 1 (units: mm).

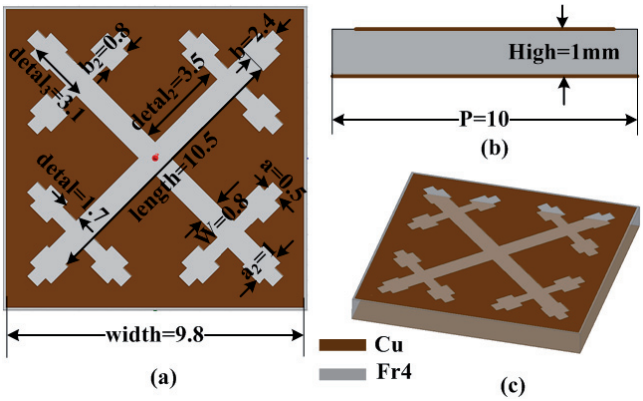

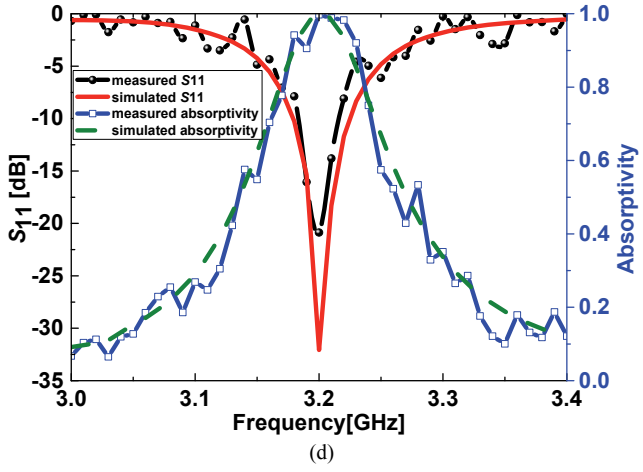

Fig. 1. Geometry and simulated absorptivity for the miniaturized FPMA unite cell. (a) Top view. (b) Side view. (c) Perspective view. (d) Simulated S_{11} and absorptivity for the FPMA with the optimized parameters.

The transmission is zero ($T = 0$) due to the copper ground plate without patterning in the bottom layer. The absorptivity (A) is defined as [11], [16], [18]

$$A = 1 - R = 1 - |S_{11}|^2 \tag{1}$$

R represents the reflection of the FPMA.

The optimized absorptivity for the structure is reported in Fig. 1(d). The FPMA displays a great absorption capability. The designed idea of the FPMA is to adjust the effective $\varepsilon(\omega)$ and $\mu(\omega)$ independently by varying the dimensions of electric resonant component and magnetic resonant component in the unit cell so as to match the surface impedance to free space and achieve a large resonant dissipation at the meantime. And while, the tangent for the absorber is absorbing the microwave at the electric and magnetic resonant frequencies. Thus, the transmission and reflection are simultaneously minimized and absorption is maximized. From Fig. 1(d), we can see that the frequency range with experimental absorptivity larger than 90 % varies from 3.17 to 3.22 GHz with a FWHM of 130 MHz (3.14-3.27 GHz).

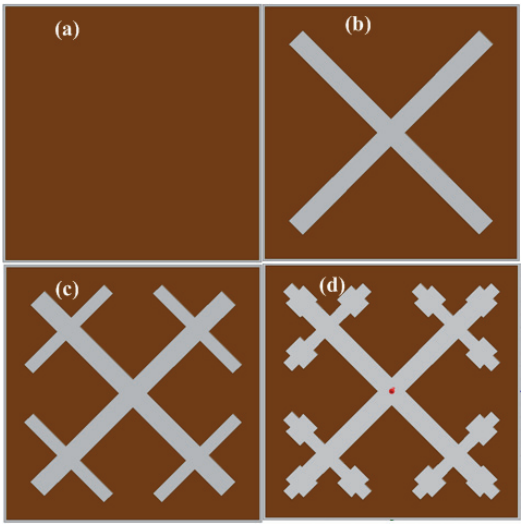

Fig. 2. Schematics of proposed fractal-shaped TOOCDS structure for FPMA under different cases. (a) Zero-order FPMA. (b) One-order FPMA. (c) Two-order FPMA. (d) Three-order FPMA.

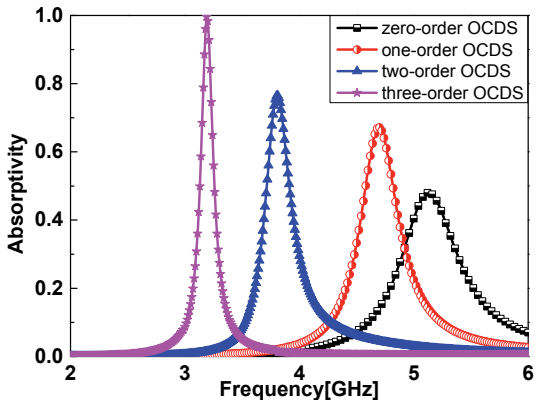

Fig. 3. Simulated results of the absorptivity for the proposed FPMA with different cases.

Fig. 2 gives the schematics of the proposed fractal TOOCDS structure under different cases and Fig. 3 shows the corresponding S_{11} results. The construction law of the fractal TOOCDS structure can be briefly described by the recursive principle as follows: in the first step, an oblique cross dipole slot (OCDS) originating from one central with a length of $detal_2$, followed by considering each end of these dipole as fresh starting points. Each of them produces a new OCDS with a length of $detal_3$. Taking this repeated procedure in a recursive fashion, the third and higher-order self-similar fractals are formed as a function factor F and iteration order n:

$$L_n = L_1/F^{(n-1)} . \quad (2)$$

Note that L_3 is selected larger than L_2/F in this particular design to guarantee the small gap space which can be adjusted to tailor the magnetic resonant frequency and accordingly facilitates a balanced condition. Parameters for the structures are same with the ones in Fig. 1. From Fig. 2 and Fig. 3, we can see that the resonance frequency shifted from 5.12 to 3.2 GHz and the absorptivity increased from 0.48 to 0.99 as the order value increased from zero to three. It is obvious that the miniaturization for the fractal TOOCDS structure has been enhanced 60 % compared with the zero-order ones.

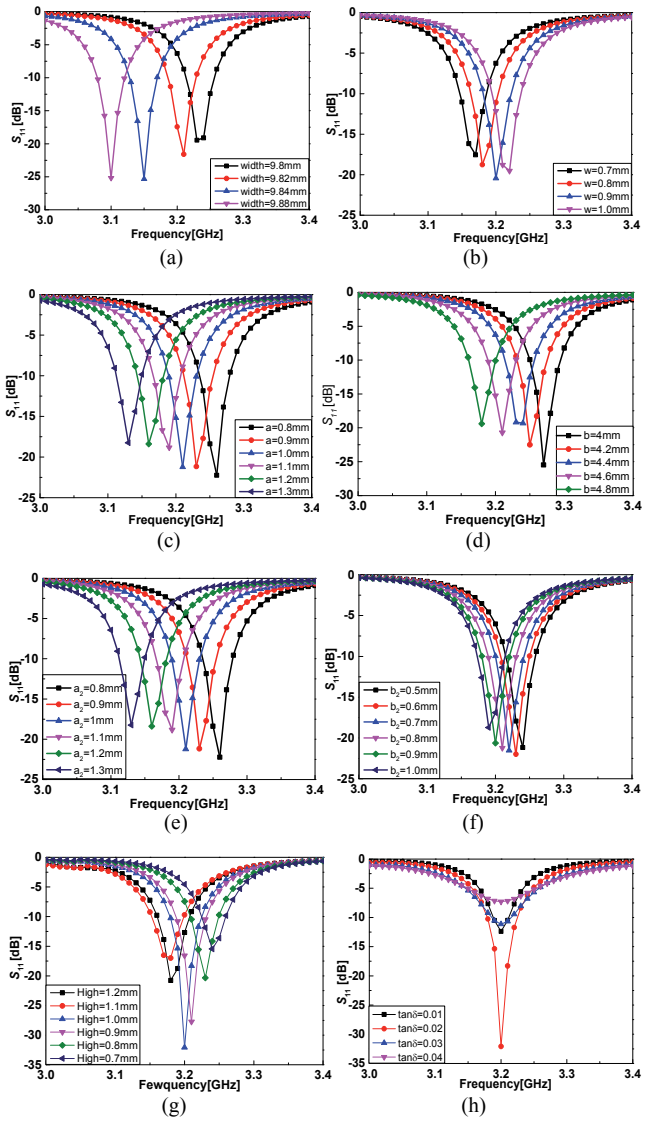

Fig. 4. The simulated results of S_{11} for the proposed FPMA with different parameters. (a) width, (b) w, (c) a, (d) b, (e) a_2, (f) b_2, (g) high, and (h) tanδ.

A parametric study was carried out and the simulated results for the proposed FPMA with different values of width, w, a, b, a_2, b_2, high and tanδ is shown in Fig. 4. In the process of the study, the metallic layers were assumed to zero-thickness for reducing the computation time. It can be seen that the resonance frequency will be decreased as the width, a, b, a_2 and b_2 increase. The resonance frequency is increased as w changes from 0.7 to 1 mm. The optimized height is 1 mm. From Fig. 4, the b_2 is the minimum amount of elements that have to be illuminated to excite the absorber. The resonance frequency should be 3.2 GHz for its application on the RCS reduction for GSAAs and the S_{11} is minimized as the parameters optimization. The optimized parameters are shown in Fig. 1.

3. RCS Reduction of GSAAs

In this section, the ultrathin and miniaturized FPMA has been applied for RCS reduction on the GSAAs. The surface current distribution of the GSAAs is analyzed and the metal surface of the GSAAs is divided into the strong current area and the weak current area. The FPMA has been loaded on the weak current area for RCS reduction of the array antennas and the metal surface with the strong current is simultaneously retained to avoid the radiation deterioration. The geometry and the surface current distribution of the 1×10 GSAAs are shown in Fig. 5. The strong surface current area of the array antennas is near the two sides of the slots and the weak surface current area is around the array antennas from Fig. 5(d). So the FPMA is loaded on the weak current area to avoid the radiation deterioration in Fig. 6. The distance between the slots and the FPMA is optimized from 1 to 5 mm to minimize the gain reduction, and the optimized result is 3 mm.

To demonstrate the GSAAs loaded the proposed FPMA, an intensive simulation study is carried out and the results are discussed. Fig. 7. shows the simulated S_{11} and gain. The impedance bandwidth of 2.2 % (S_{11} < -10 dB) from 3.15 to 3.22 GHz is achieved for the common antennas (which is the GSAAs without FPMA) and the antennas loaded the FPMA obtained an impedance bandwidth of 2.25 % from 3.15 to 3.23 GHz, from which it can be found that the two antennas have the same resonant frequency. The gain, shown in Fig. 7, varies from 13.6 to 14.5 dBi for the two antennas at the working frequency (3.15 GHz to 3.23 GHz). The antennas loaded FPMA obtain a gain of 14.1 dBi, which are 0 to 0.68 dB lower than that of common antennas from 3.15 to 3.2 GHz and higher than that from 3.2 to 3.23 GHz. The radiation characters of the GSAAs loaded FPMA can be retained for the FPMA loaded on the weak surface current area.

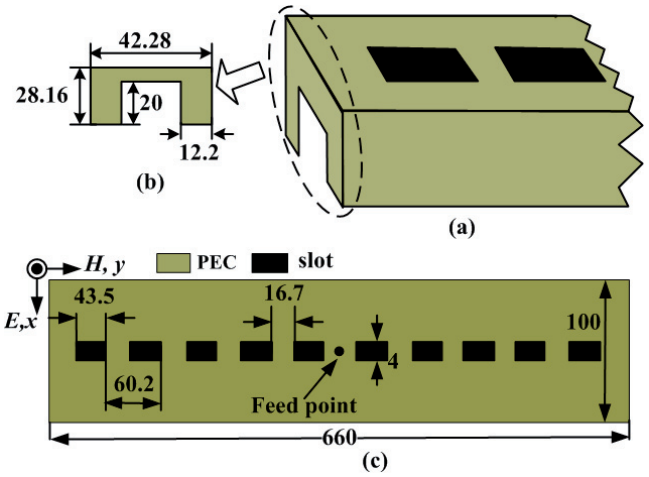

Fig. 5. The geometry and surface current distribution of the 1×10 guidewave slot array antennas (units: mm). (a) Geometry of array antennas. (b) Side view and (c) Top view for the array antennas. (d) Surface current distribution of the antennas at 0°, 90°, 180° and 270° at 3.18 GHz.

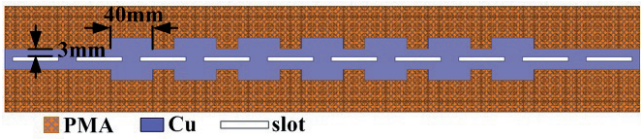

Fig. 6. The GSAAs loaded the FPMA based on the surface current distribution.

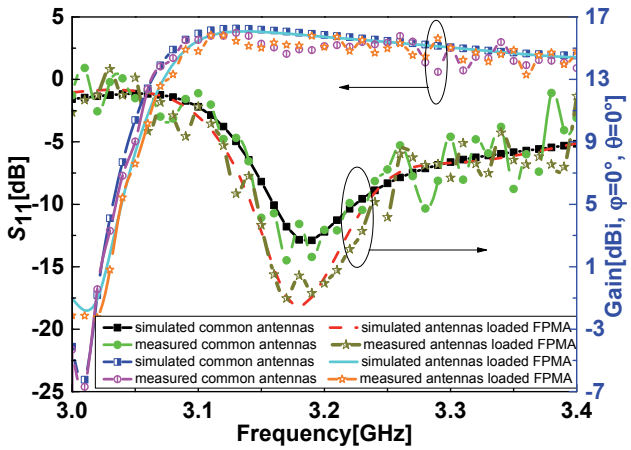

Fig. 7. Simulated S_{11} and gain for guidewave slot array antennas loaded FPMA and common antennas from 3.0 to 3.4 GHz.

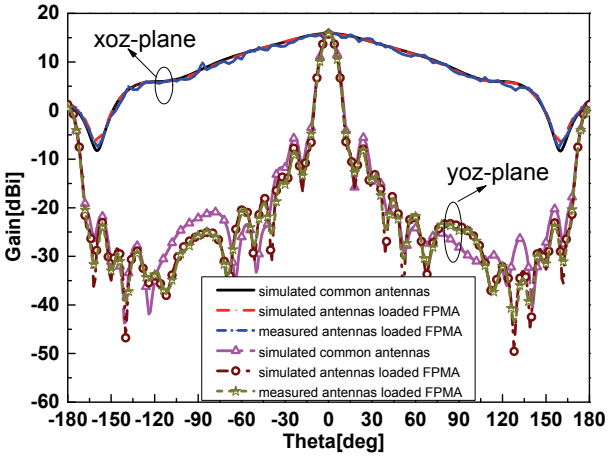

Fig. 8. Radiation patterns of the guidewave slot array antennas loaded FPMA and common antennas at 3.18 GHz.

Simulated radiation patterns of the array antennas at 3.18 GHz are given in Fig. 8. It can be seen that the radiation patterns of the guidewave slot array antennas loaded FPMA are the same as one of the common antennas at 3.18 GHz. The front-to-back ratio (FBR) remains to be better than 15.1 dB for the antennas loaded FPMA, which is 0.3 dB lower than that of common antennas. The radiation characters are retained compared with the common array antennas.

The simulated monostatic and bistatic RCSs of the two GSAAs are given in Fig. 9. From Fig. 9(a) and 9(b), it is found that the monostatic RCS reductions of the array antennas are significantly achieved from 3.15 to 3.25 GHz for the *x*-polarized incident wave and *y*-polarized incident wave. The GSAAs have -26.2 dB of RCS reduction peaks for the *x*-polarized incident wave at 3.2 GHz and -24.5 dB of RCS reduction peaks for *y*-polarized incident wave at 3.19 GHz, respectively. The frequency shift of 10 MHz and the different peak values of RCS reductions are mainly caused by the impact of the edge diffraction along the X axis and the Y axis. Fig. 9(c) and 9(d) present the simulated bistatic RCS for the common antennas and the array antennas loaded FPMA with the x- and y-polarized incident waves at 3.2 GHz. From Fig. 9(c), it can be found that

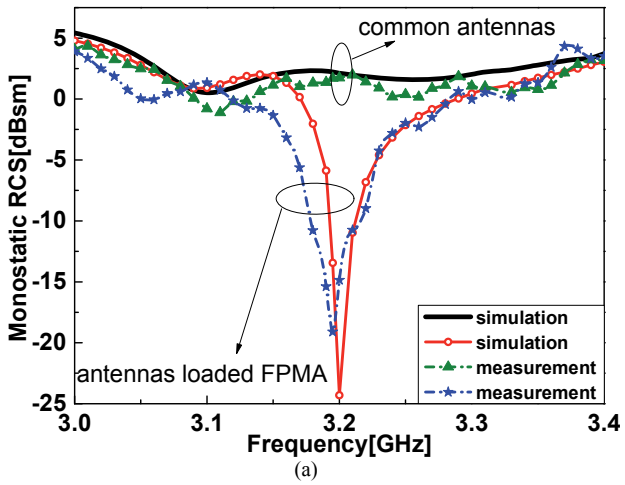

(a)

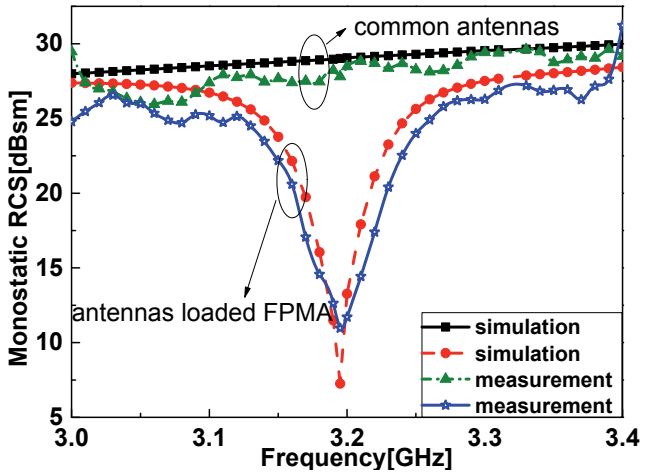

(b)

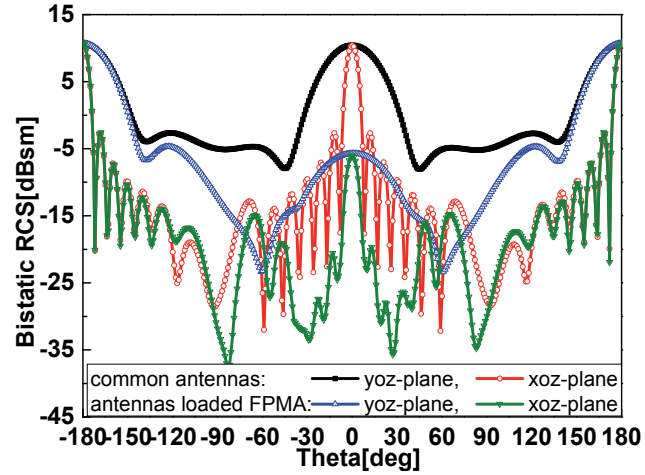

(c)

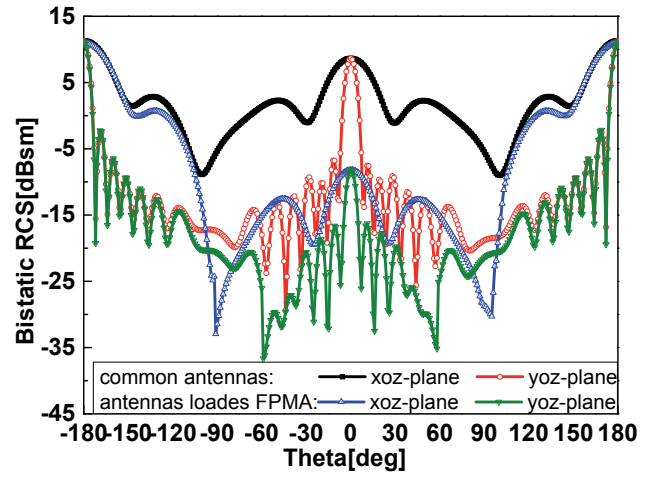

(d)

Fig. 9. Comparison of monostatic and bistatic RCS of the GSAAs loaded FPMA and common antennas. Simulated and measured monostatic RCS reduction with (a) *x*-polarized incident wave and (b) *y*-polarized incident wave impinging from normal direction. Simulated results of the bistatic RCS for antennas loaded FPMA with (c) *x*-polarized incident wave and (d) *y*-polarized incident wave at 3.2 GHz.

for the case of *x*-direction polarized incident wave, the bistatic RCS has been effectively reduced in angular ranges of [-110°, -80°] and [-50°, 50°] in xoz-plane, and [-110°, 110°] in yoz-plane. From Fig. 9(d), we find the RCS has been effectively reduced in angular ranges of [-110°, 110°] in xoz-plane, and [-90°, 90°] in yoz-plane for *y*-direction polarized incident wave.

4. Fabrication and Measurement

To verify the simulation results, the prototypes of the FPMA, the proposed GSAAs loaded FPMA and the common array antennas are illustrated in Fig. 10 and have been experimentally studied. The proposed FPMA samples were respectively fabricated using an optical lithographic processes on a 1-mm-thick FR4 substrate with $\varepsilon_r = 4.4$ and $\tan\delta = 0.02$. The waveguide method [9], [11], [18] (closed system) has been used to verify the absorption. The measured results are shown in Fig. 1(d). The measured absorptivity larger than 90 % varies from 3.17 to 3.22 GHz with a FWHM of 110 MHz (3.14-3.25 GHz).

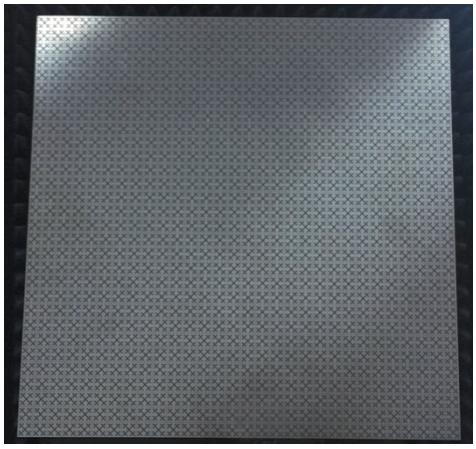

(a)

(b)

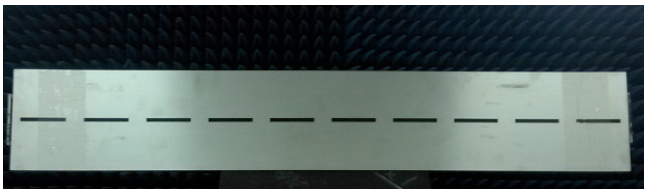

(c)

Fig. 10. The prototypes of array antennas. (a) The proposed FPMA. (b) The proposed guidewave slot array antennas loaded the FPMA. (c) The common array antennas.

The experimental S_{11} and gain are given in Fig. 7. As seen from the curve, the array antennas loaded the FPMA have a narrow impedance bandwidth of 2.5 % from 3.15 to

3.23 GHz. The proposed array antennas obtain an average gain value of 13 dBi across the operating bandwidth from 3.15 to 3.23 GHz and the gain reduction is less than 0.73 dB. The experimental results indicate that the reliability of the loaded FPMA for array RCS reduction is based on its surface current distribution. Fig. 8 shows the experimental radiation patterns results at 3.18 GHz for both the xoz-plane and yoz-plane. The patterns are stable cross the operating bandwidth. The FBR remains to be better than 10.5 dB for the antennas loaded the FPMA, which is 0.9 dB lower than that of common antennas.

The measured results of the monostatic RCS for two types of array antennas are shown in Fig. 9(a) and (b). The array antennas samples respectively have the monostatic RCS reduction peaks of -22.8 dB at 3.19 GHz for *x*-polarized incident wave and -20.1 dB at 3.2 GHz for *y*-polarized incident wave. The measured results indicate that the array antennas loaded FPMA significantly obtain the RCS reduction from 3.15 to 3.25 GHz for both the *x*-polarized and *y*-polarized incident wave. The measured and simulated results are in good agreement.

It is necessary to point out that the presented FPMA has the advantages of ultra-thin and miniaturized structure and perfect absorption. However, the limitation of the FPMA is narrow bandwidth of absorption. So the next work is to enhance the bandwidth of absorption for the FPMA.

5. Conclusion

In this paper, a fractal three-order oblique cross dipole slot structure is presented to miniaturize the PMA and the fractal metamaterial perfect absorber is loaded on the guidewave slot array antennas to reduce their in-band RCS. The surface current distribution of the array antennas divided into the strong and weak current areas is presented. The FPMA is only loaded on the weak current area. The RCS of the 1×10 guidewave slot array antennas is reduced. Simulated *S*-parameters, radiation patterns, gain, directivity, and RCS reduction of the array antennas are compared with the measured results. Measured results indicated that the in-band RCS of the array antennas loaded the FPMA has been dramatically reduced and the gain reduction is only about 0.73 dB. Experimentally and theoretically, it can be observed that the proposed FPMA has the advantages of the ultra-thin and miniaturized structure, the perfect absorption and the high RCS reduction. The next work is to enhance the bandwidth of absorption for the fractal metamaterial perfect absorber.

Acknowledgements

Authors thank the supports from the National Natural Science Foundation of China under Grant (No.61271100, No.61471389), Natural Science Foundational Research Fund of Shannxi Province (No.2010JZ6010 and No.2012JM8003), and the Doctoral Foundation Air Force Engineering University under Grant (No.KGD080914002). They also thank the reviewers for their valuable comments.

References

[1] GENOVESI, S., COSTA, F., MONORCHIO, A. Wide band radar cross section reduction of slot antennas arrays. *IEEE Trans. Antennas Propag.*, 2014, vol. 62, no. 1, p. 163–173.

[2] WENBO PAN, CHENG HUANG, PO CHEN, XIAOLIANG MA, CHENGGANG HU, XIANGANG LUO. A low-RCS and high-gain partially reflecting surface antenna. *IEEE Trans. Antennas Propag.*, 2014, vol. 62, no. 2, p. 945–949.

[3] ZHOU, H., QU, S.-B., LIN, B.-Q. Filter-antenna consisting of conical FSS radome and monopole antenna. *IEEE Trans. Antennas Propag.*, 2012, vol. 60, no. 6, p. 3040–3045.

[4] GENOVESI, S., COSTA, F., MONORCHIO, A. Low profile array with reduced radar cross section by using frequency selective surfaces. *IEEE Trans. on Antennas and Propagation*, 2012, vol. 60, no. 5, p. 2327–2335.

[5] LI, Y.-Q., ZHANG, H., FU, Y.-Q., YUAN, N.-C. RCS reduction of ridged waveguide slot antenna array using EBG radar absorbing material. *IEEE Antennas Wireless Propag. Lett.*, 2008, vol. 7, p. 473–476.

[6] TAN, Y., YAN, N., YANG, Y., FU, Y. Improved RCS and efficient waveguide slot antenna. *Electron. Lett.*, 2011, vol. 47, no. 10, p. 582–583.

[7] ZHANG, Y., MITTER, R., WANG, B. Z., HUANG, N. T. AMCs for ultra-thin and broadband RAM design. *Electron. Lett.*, 2009, vol. 45, no. 10, p. 484–485.

[8] HWANG, R. B., TSAI, Y. L. The reflection characteristics of a composite planar AMC surface. *Applied Phys. Lett. Advances*, 2012, no. 2, p. 012128.

[9] ZHAO, Y., CAO, X. Y., GAO, J., LI, W. Q. Broadband RCS reduction and high gain waveguide slot antenna with orthogonal array of CSRR-AMC. *Electron. Lett.*, 2013, vol. 49, no. 21, p. 1312-1313.

[10] IRIARTE GALARREGUI, J. C., TELLECHEA PEREDA, A., MARTINEZ DE FALCON, J. L., EDERRA, I., GONZALO, R., DE MAAGT, P. Broadband radar cross-section reduction using AMC technology. *IEEE Trans. Antennas Propag.*, 2013, vol. 61, no. 12, p. 6136-6143.

[11] LANDY, N. I., SAJUYIGBE, S., MOCK, J. J., SMITH, D. R., PADILLA, W. J. A perfect metamaterial absorber. *Phys. Rev. Lett*, 2008, vol. 100, p. 207402.

[12] LONG LI, YANG YANG, CHANGHONG LIANG. A wide-angle polarization-insensitive ultra-thin metamaterial absorber with three resonant modes. *J. Appl. Phys.*, 2011, vol. 110, p. 063702.

[13] LI SI-JIA, CAO XIANG-YU, GAO JUN, ZHENG QIU-RONG, ZHAO YI, YANG QIN. Design of ultrathin broadband perfect metamaterial absorber with low radar cross section. *Acta Phys. Sin.*, 2013, vol. 62, no. 19, p. 194101.

[14] WANGREN XU, SONKUSALE, S. Microwave diode switchable metamaterial reflector/absorber. *Applied Phys. Lett.*, 2013, vol. 103, p. 0301902.

[15] DEXIN YE, ZHENG WANG, ZHIYU WANG, KUIWEN XU, BIN ZHANG, JIANGTAO HUANGFU, CHANGZHI LI, LIXIN RAN. Towards experimental perfectly-matched layers with ultra-

thin metamaterial surfaces. *IEEE Trans. Antennas Propag.*, 2013, vol. 60, no. 11, p. 5162–5172.

[16] LIU, T., CAO, X. Y., GAO, J., ZHENG, Q. R., LI, W. Q., YANG. H. H. RCS reduction of waveguide slot antenna with metamaterial absorber. *IEEE Trans. Antennas Propag.*, 2013, vol. 61, no. 4, p. 2327–2335.

[17] SIJIA LI, XIANGYU CAO, TAO LIU, HUANHUAN YANG. Double-layer perfect metamaterial absorber and its application for RCS reduction of antenna. *Radioengineering*, 2014, vol. 23, no. 1, p. 222–228.

[18] SIJIA LI, JUN GAO, XIANGYU CAO, ZHAO ZHANG. Loaded metamaterial perfect absorber using substrate integrated cavity, *J. Appl. Phys.*, 2014, vol.115, p. 213703.

[19] HE-XIU XU, GUANG-MING WANG, MEI-QING QI, JIAN-GANG LIANG, JIAN-QIANG GONG, ZHI-MING XU. Triple-band polarization-insensitive wide-angle ultra-miniature metamaterial transmission line absorber. *Phys. Rev. B*, 2012, vol. 86, p. 205104.

[20] SIJIA LI, JUN GAO, XIANGYU CAO, WENQIANG LI, ZHAO ZHANG, DI ZHANG. Wideband, thin and polarization-insensitive perfect absorber based the double octagonal rings metamaterials and lumped resistances. *J. Appl. Phys.,* 2014, vol. 116, p. 043710.

About Authors ...

Sijia LI was born in Xi'an, Shaanxi province, P.R. China in 1987. He received the B. Eng. degree in Electronics and Information Engineering from Guangxi University, Nanning, China, in 2009 and the M. Eng. degree in Information and Telecommunication Engineering from Air Force Engineering University, Xi'an China, in 2011. He is currently working toward Ph.D degree in Electronic Science and Technology at the Information and Navigation college of Air Force Engineering University. He has been working with the Military Communication and Navigation Antenna and EMC Lab., since 2012. His research activity has been focused in the broadband and fractal perfect metamaterial absorber and its application for RCS reduction of antennas. He has authored and coauthored more than 40 scientific papers in major journals and international conferences. He received the excellent Master's dissertation in 2012. He is awarded the 2012 and 2013 Best Student Paper Prize (First Prize) of the National Graduate Mathematical Modeling Contest in Shanghai in December 2012 and in Changsha in December 2013. He was a recipient of the Best Paper Award at the Forth National Doctor Forum Symposium on Information Science of China in Guangzhou in October 2013. He is awarded the excellent student in the 2014 national summer school of the Microwave Material and Components. He is a reviewer of the Applied Physics Letter, Journal of Applied Physics, Transactions on Microwave Theory & Techniques, IEEE Transactions on Antennas & Propagation, and Microelectronics Journal.

Xiangyu CAO received the B. Sc and M.A. Sc degrees from Air Force, the Missile Institute in 1986 and 1989, respectively. She joined the Air Force Missile Institute in 1989 as an assistant teacher. She became an associate professor in 1996. She received Ph.D. degree in Missile Institute of Air Force Engineering University in 1999. From 1999 to 2002, she was engaged in postdoctoral research in Xidian University, China. She was a Senior Research Associate in the Dept. of Electronic Engineering, City University of Hong Kong from June 2002 to Dec 2003. She is currently a professor of Information and Navigation college of Air Force Engineering University of CPLA. She is the IEEE senior member from 2008. She has authored and coauthored more than 200 technical journal articles and conference papers, and holds one China soft patent. She is the coauthor of two books entitled, Electromagnetic Field and Electromagnetic Wave, and Microwave Technology and Antenna published in 2007 and 2008, respectively. Her research interests include smart antennas, electromagnetic metamaterial and their antenna applications, and electromagnetic compatibility. She is a reviewer of Applied Physics Letter, Journal of Applied Physics, IEEE Transactions on Antennas & Propagation, and IEEE Antennas Wireless Propagation Letter.

Jun GAO received the B.Sc and M.A.Sc degrees from Air Force the Missile Institute in 1984 and 1987, respectively. He joined the Air Force Missile Institute in 1987 as an assistant teacher. He became an associate professor in 2000. He is currently a professor of Information and Navigation College, Air Force Engineering University of CPLA. He has authored and coauthored more than 100 technical journal articles and conference papers, and holds one China soft patent. His research interests include smart antennas, electromagnetic metamaterial and their antenna applications.

Yuejun ZHENG was born in Yushan, Jiangxi province, in 1989. He graduated from Air Force Engineering University and received the B. S. degree in 2012. He is now a graduate student. His main research orientation is antenna radiation ameliorated and RCS reduction based on the metamaterial.

Di ZHANG was born in Baoding, Hebei province, in 1991. He received the B. S. degree from the Information and Navigation College, Air Force Engineering University in 2013. He is now a graduate student. His research interest is in electromagnetic metamaterial.

Hongxi LIU was born in Baotou, Inner Mongolia Autonomous Region, P. R. China in 1989. He received the B.S. degree in Electronic and Communication Engineering. Currently, He is now a graduate student. His recent research interests include the design of perfect metamaterial absorber design, and end-fire antennas.